



Predictions for the $(n, 2n)$ reaction cross section based on a Bayesian neural network approachW. F. Li (李伟峰),¹ L. L. Liu (刘丽乐),² Z. M. Niu (牛中明) ^{1,*} Y. F. Niu (牛一斐) ^{3,4} and X. L. Huang (黄小龙)²¹*School of Physics and Optoelectronic Engineering, Anhui University, Hefei 230601, China*²*China Nuclear Data Center, China Institute of Atomic Energy, Beijing 102413, China*³*School of Nuclear Science and Technology, Lanzhou University, Lanzhou 730000, China*⁴*MOE Frontiers Science Center for Rare Isotopes, Lanzhou University, Lanzhou 730000, China*

(Received 4 December 2023; revised 31 January 2024; accepted 1 April 2024; published 22 April 2024)

Nuclear $(n, 2n)$ reaction cross sections are studied based on the Bayesian neural network (BNN) approach. Three physical quantities besides the proton and neutron numbers are proposed to improve the performance of the BNN approach. These three physical quantities are the incident neutron energy with respect to the reaction threshold, the physical quantity related to the odd-even effect, and the theoretical $(n, 2n)$ reaction cross section, and they are included as the inputs to the neural network. The BNN approach has better performance in the description of the $(n, 2n)$ reaction cross sections than the theoretical library TENDL-2021 calculated by the TALYS code based on the Hauser-Feshbach statistical model, especially for heavy nuclei. The root-mean-square deviation of the BNN approach with respect to the evaluation data is reduced to 0.10 barns compared to 0.25 barns of TENDL-2021. The extrapolation ability of the BNN approach is verified with the $(n, 2n)$ cross section data that are not used to train the neural network. Furthermore, it is found that the BNN approach still well describes the trend of the $(n, 2n)$ cross sections with the incident neutron energy predicted by TENDL-2021 even when extrapolated to the unknown region.

DOI: [10.1103/PhysRevC.109.044616](https://doi.org/10.1103/PhysRevC.109.044616)**I. INTRODUCTION**

Nuclear data, especially neutron nuclear data, serve as an important bridge between the basic research of nuclear physics and the application of nuclear engineering and nuclear technology [1–3]. Neutron nuclear reactions play an essential role in reactor physics, and are among the most important tools for studying nuclear structure and nuclear reaction mechanics.

The $(n, 2n)$ reaction is one of the common reaction channels for neutron nuclear reactions, an important form of neutron multiplication when the incident neutron energies are typically less than about 15 MeV. It plays important roles in neutron sources, neutron scattering experiments, and neutron irradiation studies [4,5]. In recent decades, the cross sections of $(n, 2n)$ reactions have been measured by the activation method [6–9], offline γ -ray spectroscopy [10–13], the recoil method [14], etc. The most comprehensive international database of nuclear reaction experiments is the computerized interactive identifiable database EXFOR (EXchange FORmat), established through the formal international cooperation under the leadership of the International Atomic Energy Agency, which collects the experimental data on different types of nuclear reactions by different groups [15,16]. However, there are sometimes remarkable discrepancies among experimental data of nuclear reaction cross sections from different groups, making these data difficult to use directly.

Nuclear data evaluation is an important part of the process from the generation of nuclear data to the point where it can be practically applied, in which nuclear data are evaluated as recommended values [17]. Currently widely used databases, such as ENDF/B-VIII.0 (Evaluated Nuclear Data File) [18], JEFF-3.3 (Joint Evaluated Fission and Fusion File) [19], JENDL-5 (Japanese Evaluated Nuclear Data Library) [20], CENDL-3.2 (Chinese Evaluated Nuclear Data Library) [21], and BROND-3.1 (Russian Evaluated Nuclear Data Library) [22], provide a large amount of evaluation data for nuclear reactions.

It is impossible to measure all energy regions and reaction channels experimentally, so theoretical predictions are inevitable for the study of nuclear reactions and the application of nuclear data. Several code packages based on nuclear reaction theory have been developed, such as the famous TALYS [23], EMPIRE [24], CCONE [25], and UNF [26], which play very important roles in nuclear data evaluation. Experimentally, high-quality cross section data have been collected by the Nuclear Data Organization [27]; however, there are still remarkable deviations between the theoretical results and the experimental data. With the rapid development of modern science and technology, various applications in nuclear engineering and nuclear technology require more and more accurate cross sections of neutron nuclear reactions. Therefore, it is important to develop a new method to provide more accurate excitation functions of neutron nuclear reactions.

In recent years, machine learning has made impressive achievements in many areas and is currently one of the hottest and fastest-growing fields in science and technology [28]. It provides a powerful tool for physics research, is powerful in

*zmnui@ahu.edu.cn

extracting relevant features of complex nonlinear systems, and can be used to solve some complex physics problems that are difficult or temporarily intractable by traditional methods. The combination of machine learning and physics is an emerging interdisciplinary frontier that has attracted much attention in recent years. It has been applied in areas such as particle physics [29–31], condensed matter physics [32,33], and astrophysics [34,35]. In nuclear physics, machine learning methods are also widely used to study various nuclear properties [36], such as nuclear masses [37–42], charge radii [43,44], α and β decays [45–47], low-lying excitation spectra [48,49], and neutron-induced nuclear reactions [50–53].

Compared to traditional machine learning methods, the Bayesian neural network (BNN) approach can automatically avoid overfitting by introducing a prior and quantify the uncertainties in model predictions, making it one of the most important approaches for studying nuclear physics. The BNN approach has been widely used in studying various nuclear properties [54–64]. These neural network approaches can generally achieve much better accuracy than nuclear theoretical models and even provide reliable extrapolation predictions by carefully designing their architectures to incorporate more and more physical information. However, nuclear models used in TALYS etc. are based on physical background and are sometimes more realistic. Therefore, the physics behind nuclear models is important for studying the $(n, 2n)$ reaction. In this work, we improve the model predictions of the $(n, 2n)$ reaction by introducing the theoretical results predicted by TALYS into the input layer of the neural network, thus introducing the corresponding physical effects. Furthermore, the TALYS predictions are also used to test the extrapolation ability of the neural network. Special attention is paid to the design of the neural network architecture, in order to achieve a good description of the $(n, 2n)$ reaction excitation function as well as reliable extrapolation predictions. The BNN approach is briefly introduced in Sec. II. The corresponding results are presented in Sec. III. Finally, a summary and perspectives are given in Sec. IV.

II. THEORETICAL FRAMEWORK

Similarly to Ref. [54], the probability distribution $p(\omega)$ of model parameter ω in the BNN approach is introduced based on our background knowledge, which is called the prior distribution. Given a data set $D = \{(\mathbf{x}_1, o_1), (\mathbf{x}_2, o_2), \dots, (\mathbf{x}_N, o_N)\}$, the prior distribution $p(\omega)$ is updated by Bayes' theorem:

$$p(\omega|D) = \frac{p(D|\omega)p(\omega)}{p(D)} \propto p(D|\omega)p(\omega), \quad (1)$$

where \mathbf{x}_k and o_k ($k = 1, 2, \dots, N$) are the input and output data, respectively, and N is the number of data. $p(D|\omega)$ is the conditional probability that describes the impact of the data D on the prior distribution $p(\omega)$. $p(\omega|D)$ is the probability distribution of the parameters ω after the data D is given, which is called the posterior distribution. $p(D)$ is a normalization constant to ensure that the integral of posterior distribution $p(\omega|D)$ over the whole space of model parameters ω is 1.

The conditional probability $p(D|\omega)$ is usually taken to be a Gaussian distribution, which is defined as $p(D|\omega) = \exp(-\chi^2/2)$, where χ^2 is denoted by

$$\chi^2 = \sum_{k=1}^N \left(\frac{o_k - y(\mathbf{x}, \omega)}{\Delta o_k} \right)^2. \quad (2)$$

Here, Δo_k is the noise error associated with the k th data, and the reciprocal of its square is set to be the gamma distribution. In the BNN approach, the function $y(\mathbf{x}, \omega)$ is described in terms of a neural network, which, for a single hidden layer neural network, is represented as

$$y(\mathbf{x}, \omega) = a + \sum_j^H b_j \tanh \left(c_j + \sum_{i=1}^I d_{ji} x_i \right), \quad (3)$$

where $\mathbf{x} = \{x_i\}$, $\omega = \{a, b_j, c_j, d_{ji}\}$, H is the number of neurons in the hidden layer, and I is the number of input values.

In this work, the neural network is employed to study the $(n, 2n)$ reaction excitation function. By carefully designing the input layer of the neural network to include physical information, one can make the neural network easier and more effective for describing the $(n, 2n)$ reaction excitation functions. Through a number of trials, we found that ΔE , δ , and σ^{th} are essential for improving the prediction accuracy of the neural network besides the proton number Z and the neutron number N . The incident neutron energy E is another necessary input to determine the $(n, 2n)$ reaction excitation function, and it is usually taken as an the input of the neural network. Our studies found that there are very similar trends for the $(n, 2n)$ cross sections as a function of the difference $\Delta E = E - E_{\text{thresh}}$ between the incident neutron energy and the reaction threshold, which makes the predictions of the neural network much easier. There are remarkable differences among the $(n, 2n)$ reaction excitation functions for nuclei with different parity of (Z, N) due to the pairing effect, so a quantity related to the pairing effect δ ($\delta = 1, 0$, and -1 for even-even, odd- A , and odd-odd nuclei, respectively) is effective to uniformly describe the $(n, 2n)$ reaction excitation functions of all nuclei. It has been found that the predictive ability of the neural network can be significantly improved by introducing theoretical predictions into the input layer [65] or the output layer [54,58,61] to incorporate known physics. In this work, theoretical predictions of $(n, 2n)$ reaction cross sections σ^{th} taken from TENDL-2021 [66] are introduced into the input layer of the neural network. For simplicity, we will use BNN-I3, BNN-I4 δ , BNN-I4 σ , and BNN-I5 to denote the BNN approaches with $\mathbf{x} = (Z, N, \Delta E)$, $\mathbf{x} = (Z, N, \Delta E, \delta)$, $\mathbf{x} = (Z, N, \Delta E, \sigma^{\text{th}})$, and $\mathbf{x} = (Z, N, \Delta E, \delta, \sigma^{\text{th}})$ as inputs, respectively. The outputs of BNN-I3, BNN-I4 δ , BNN-I4 σ , and BNN-I5 are the $(n, 2n)$ reaction cross sections. The numbers of neurons in the hidden layer of the four neural networks are 210, 175, 175, and 150, respectively, which ensures that the parameters of these four neural networks are the same. As in Ref. [54], the mathematical expectation and standard deviation of the neural network output over the posterior distribution are used as the final $(n, 2n)$ cross section predictions and their uncertainties. It should be pointed out that the BNN predictions might be very small negative values when E is

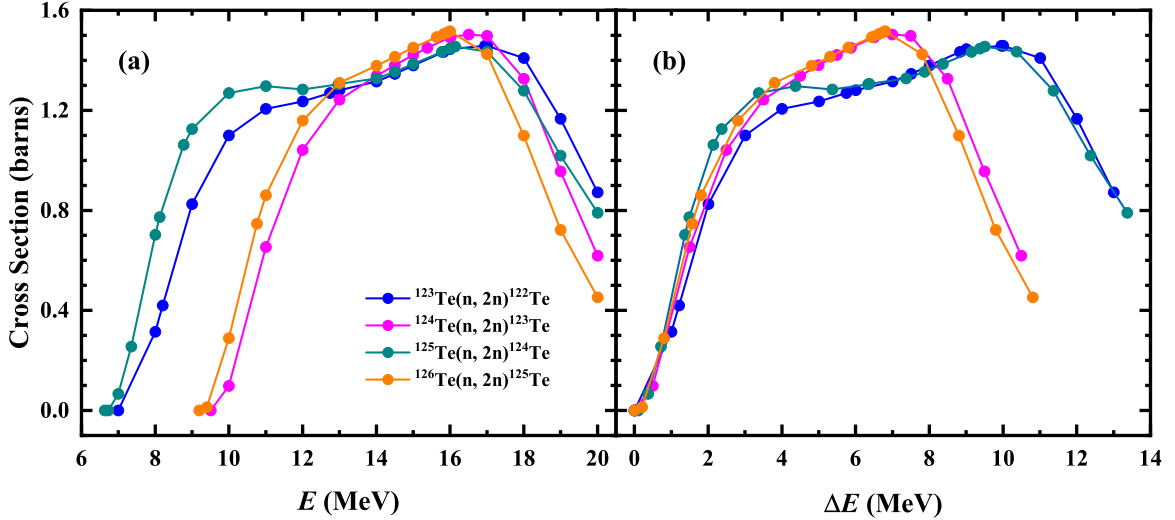


FIG. 1. The $(n, 2n)$ reaction cross sections of Te isotopes from ENDF/B-VIII.0 [18] as a function of (a) E and (b) ΔE .

very close to the threshold energy; we will take them as zero since the cross sections cannot be negative.

The $(n, 2n)$ reaction cross section evaluation data used to train the neural networks are taken from the ENDF/B-VIII.0 library for nuclei with $Z = 8-100$ [18], where only those data with the incident neutron energy below 20 MeV are considered. To check the reliability of the BNN predictions, the cross section data of four nuclei, ^{115}Ag , ^{139}Ba , ^{178}Hf , and ^{248}Cm , in the different nuclear mass regions are selected as the testing set, and the data for the remaining 515 nuclei are used as the learning and validation sets. There are remarkable deviations between the cross sections in TENDL-2021 and ENDF/B-VIII.0 for these four nuclei, which may indicate that the description of these $(n, 2n)$ reaction cross sections is relatively challenging for theoretical models. Therefore, the data of these nuclei are crucial to test the predictive ability of the neural network. If all the cross section data are used to train the neural networks, the nuclei with too much data will be heavily weighted, resulting in poor generalization of the neural network. To solve this problem, no more than 20 cross section data are taken as the learning set for each nucleus, and the remaining data are used as the validation set. The selection rule is that the cross section data at the minimum and maximum incident neutron energies are first selected, and then 18 cross sections are randomly selected from the remaining data. There are 8666, 2598, and 85 cross section data in the learning, validation, and testing sets, respectively.

The root-mean-square (rms) deviation of model predictions with respect to experimental data is usually used to evaluate the model accuracy. For the $(n, 2n)$ reaction cross section, the rms deviation is defined to be

$$\sigma_{\text{rms}}(\text{Cross Section}) = \sqrt{\sum_{i=1}^N (\sigma_i^{\text{exp}} - \sigma_i^{\text{th}})^2 / N}, \quad (4)$$

where σ_i^{exp} and σ_i^{th} are the cross sections from the evaluation data and theoretical predictions for nucleus i , and N is the number of data to be evaluated. The loss functions of neural

networks in this work are taken to be $\sigma_{\text{rms}}(\text{Cross Section})$ as well.

III. RESULTS AND DISCUSSION

There are remarkable differences in the $(n, 2n)$ reaction cross sections of nuclei with different (Z, N) parity due to the pairing effects, which means the cross sections of the neighboring isotopes of odd- Z and even- Z nuclei are remarkably different. Taking the ^{123}Te , ^{124}Te , ^{125}Te , and ^{126}Te isotopes as examples, Fig. 1(a) shows their $(n, 2n)$ reaction cross sections from ENDF/B-VIII.0 [18] as a function of E . It is clear that the energy thresholds of the $(n, 2n)$ reactions for even- N or odd- N isotopes generally decrease with increasing neutron number. If the $(n, 2n)$ reaction cross sections are described as a function of ΔE , which are shown in Fig. 1(b), the nuclear excitation function with an odd or even number of neutrons is more similar. We find that this helps the neural network to grasp the features of the $(n, 2n)$ excitation functions more efficiently. Therefore, we use ΔE as one of the input variables of the neural network instead of E .

From Fig. 1(a), the energy thresholds for even- N isotopes are remarkably larger than those for the neighboring odd- N isotopes, while their trends of cross sections with E are similar around the maxima of the excitation functions. This certainly induces an odd-even staggering of the integral $S_\sigma = \int_{E_{\text{thresh}}}^{20 \text{ MeV}} \sigma(E) dE$, which is shown in Fig. 2, taking Ag and Sn isotopes as examples. It can be clearly seen that the $(n, 2n)$ reaction cross sections for both Ag and Sn isotopes have a clear odd-even staggering, i.e., regardless of whether the proton number is odd or even. Therefore, introducing the δ input helps to improve the performance of the neural network.

Figure 3 shows the rms deviations $\sigma_{\text{rms}}(\text{Cross Section})$ of different BNN predictions with respect to the evaluation data [18] of $(n, 2n)$ reaction cross sections for the total set, learning set, validation set, and testing set. It can be seen that four BNN approaches all describe the $(n, 2n)$ reaction cross section better than the TENDL-2021 [66]. The BNN-I5 approach achieves the best accuracy for the learning set, validation

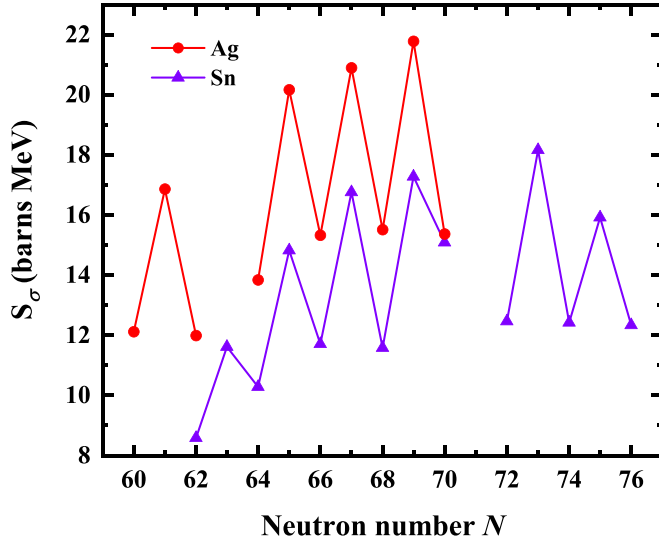


FIG. 2. The integral S_σ of the cross sections with respect to E for Ag and Sn isotopes.

set, and testing set, which indicates that adding the relevant physical quantities to the input of the neural network can improve the performance of the BNN approaches. Therefore, only BNN-I5 predictions are given hereafter.

The scatter distribution of the $(n, 2n)$ reaction cross sections predicted by the BNN-I5 approach and TENDL-2021 as a function of their evaluation data is shown in Fig. 4. It can be seen that the $(n, 2n)$ reaction cross sections are generally within 2.5 barns. The TENDL-2021 describes the $(n, 2n)$ reaction cross sections well, while its description is relatively poor for small cross sections. For cross section data smaller than 0.5 barns, approximately 15% of the TENDL-2021 predictions deviate from the evaluation data by larger

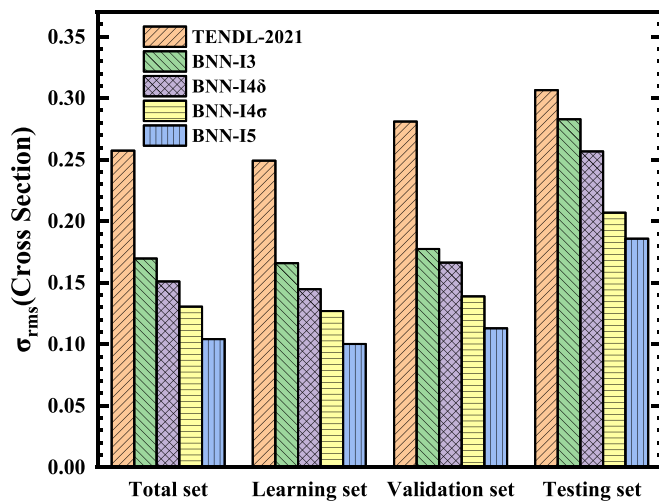


FIG. 3. The rms deviations σ_{rms} (Cross Section) of different BNN predictions with respect to the evaluation data [18] of $(n, 2n)$ reaction cross sections for the total set, learning set, validation set, and testing set. The corresponding σ_{rms} (Cross Section) of TENDL-2021 [66] are shown for comparison.

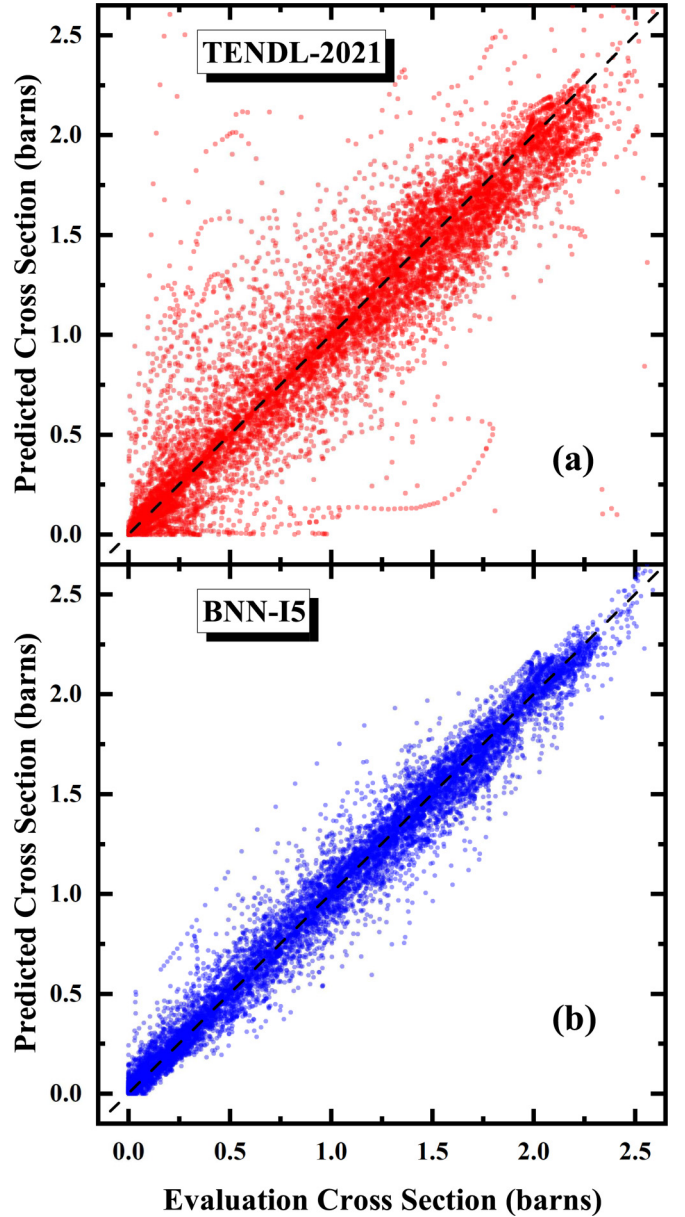


FIG. 4. Scatter distribution of the $(n, 2n)$ reaction cross sections predicted by the BNN-I5 approach and TENDL-2021 [66] as a function of the evaluation data.

than 0.2 barns, with some predictions even deviating by over 2 barns. In comparison, the BNN-I5 approach is better than the TENDL-2021 in describing the reaction cross sections not only for the large cross sections but also for the small cross sections. Only 8% of the BNN-I5 predictions deviate from the evaluation data by larger than 0.2 barns. In order to study the predictive ability of the BNN-I5 approach for the $(n, 2n)$ reaction cross sections in different nuclear mass regions, its rms deviations σ_{rms} (Cross Section) with respect to the evaluation data in different nuclear regions are shown in Fig. 5 and compared with TENDL-2021 [66]. It is clear that the prediction accuracies of BNN-I5 are much better than those of TENDL-2021 in all nuclear mass regions. Furthermore,

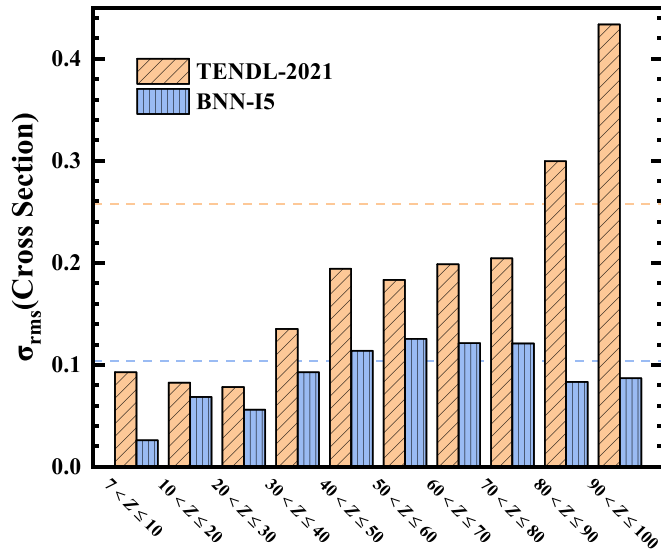


FIG. 5. The rms deviations σ_{rms} (Cross Section) of cross section predictions by BNN-I5 and TENDL-2021 [66] with respect to the evaluation data in different nuclear regions. The dashed line shows the corresponding rms deviations of the total set.

the σ_{rms} (Cross Section) of TENDL-2021 becomes larger and larger for the heavier nuclei. However, the BNN-I5 approach has a similar prediction accuracy in the whole nuclear region. This indicates that the BNN-I5 approach can describe the $(n, 2n)$ reaction cross sections better than TENDL-2021, especially for the heavy nuclei.

Taking ^{61}Ni , ^{88}Sr , ^{100}Mo , ^{135}I , ^{145}Pm , and ^{184}Os as examples, the $(n, 2n)$ reaction cross sections predicted by the BNN-I5 approach are shown in Fig. 6. The evaluation data and TENDL-2021 results [66] are also given for comparison. It is clear that the BNN-I5 approach describes well the trend of first increasing and then decreasing for the $(n, 2n)$ reaction excitation functions. Furthermore, BNN-I5 reproduces well the $(n, 2n)$ reaction cross sections for both the learning and validation sets. For ^{61}Ni and ^{145}Pm , the BNN-I5 predictions are similar to those of TENDL-2021. For ^{88}Sr , ^{135}I , and ^{184}Os , TENDL-2021 underestimates the cross sections when E is larger than about 15, 16, and 12 MeV, respectively. For ^{135}I and ^{100}Mo , the TENDL-2021 overestimates the cross sections when E is smaller than about 15 MeV and larger than about 18 MeV, respectively. However, the BNN-I5 approach removes well these deviations of TENDL-2021 with respect

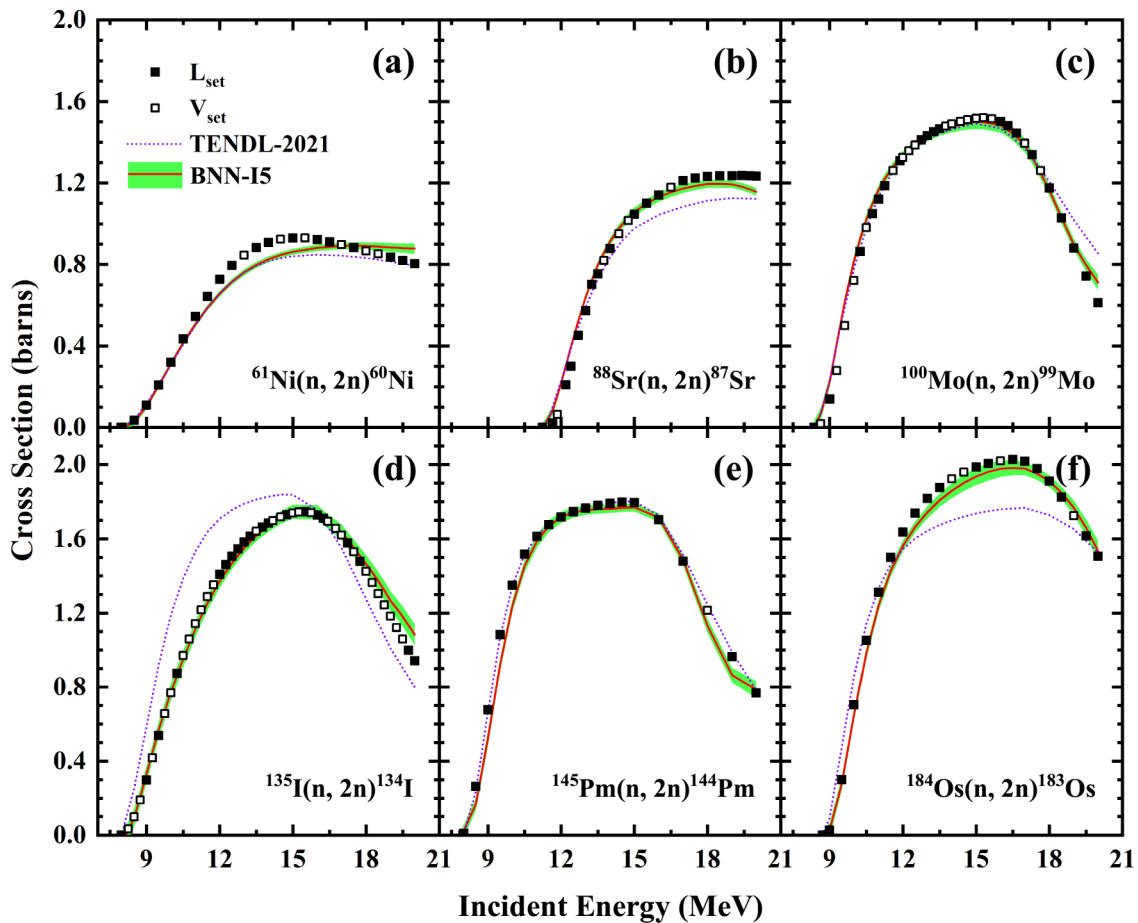


FIG. 6. The $(n, 2n)$ reaction cross sections predicted by the BNN-I5 approach for ^{61}Ni , ^{88}Sr , ^{100}Mo , ^{135}I , ^{145}Pm , and ^{184}Os . The evaluation data in the learning and validation sets are indicated by the filled squares and open squares, respectively. The BNN-I5 predictions and their uncertainties are shown as the solid lines and green hatched regions. The theoretical results from TENDL-2021 [66] are shown by the dotted lines for comparison.

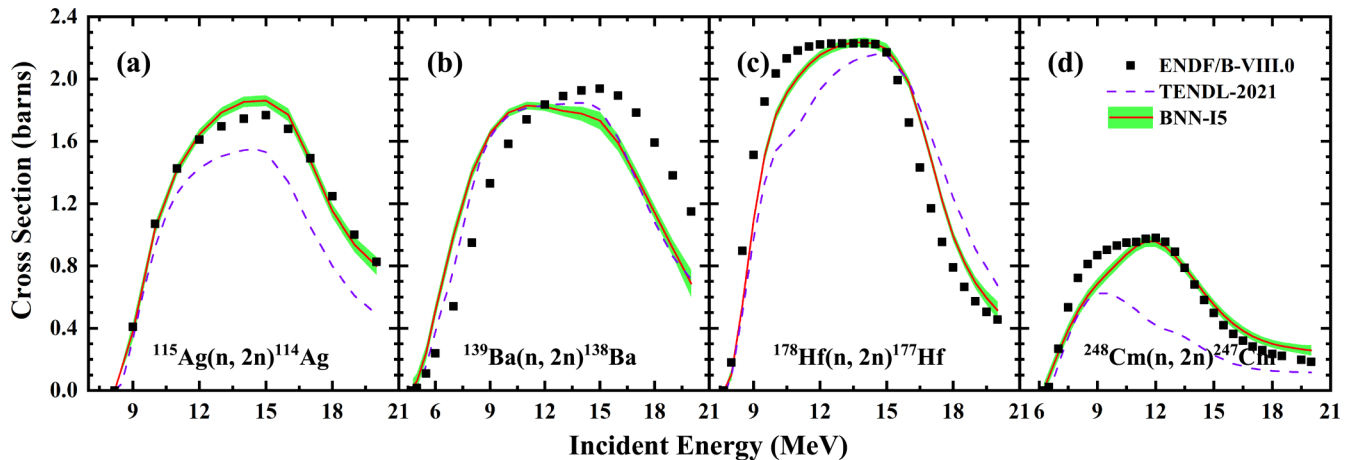


FIG. 7. Same as Fig. 6, but for ^{115}Ag , ^{139}Ba , ^{178}Hf , and ^{248}Cm .

to the evaluation data, and hence remarkably improves the $(n, 2n)$ reaction excitation functions for ^{88}Sr , ^{100}Mo , ^{135}I , and ^{184}Os .

The cross section data in the testing set, i.e., those of ^{115}Ag , ^{139}Ba , ^{178}Hf , and ^{248}Cm , can be used to verify the predictive ability of the BNN-I5 approach, since these data are not used in the learning and validation sets. Figure 7 shows the $(n, 2n)$ reaction cross sections predicted by the BNN-I5 and TENDL-2021 for these nuclei. It can be seen that the BNN-I5 approach describes the $(n, 2n)$ reaction excitation functions for ^{115}Ag , ^{178}Hf , and ^{248}Cm better than TENDL-2021. For ^{139}Ba , the BNN-I5 predictions are similar to TENDL-2021, which both overestimates the cross sections when $E \lesssim 12$ MeV and underestimates the cross sections when $E \gtrsim 12$ MeV. To further test the extrapolation ability of the BNN-I5 approach in the unknown neutron-rich region, the BNN-I5 predictions are extrapolated from the known region in two steps. Taking Na, Ca, Ge, Sb, Tb, Hf, Pb, and U isotopes ranging from the light, medium nuclei to the heavy nuclei as examples, the corresponding results are shown in Fig. 8. For these nuclei without evaluation data, the uncertainties of the BNN-I5 predictions gradually increase, while the BNN-I5 approach still well describes the trend of first increasing and then decreasing for the $(n, 2n)$ reaction excitation functions. The BNN-I5 predictions are generally larger than TENDL-2021 for light nuclei, e.g., Na isotopes. In the heavy nuclear region, there are large deviations between the BNN-I5 and the TENDL-2021 predictions, e.g., in U isotopes. As shown in Fig. 5, BNN-I5 is powerful in the learning set, while the BNN approach generally becomes less reliable for the extrapolation. It also should be pointed out that the TENDL-2021 results predicted by TALYS based on the physical background would be more realistic for the extrapolation.

Taking ^{66}Zn , ^{144}Sm , and ^{192}Pt as examples, Fig. 9 shows the comparison between the $(n, 2n)$ reaction cross sections predicted by the BNN-I5 approach and the original experimental data, which are obtained directly from measurements and have not been evaluated [67–91]. Clearly, the experimental data from different groups can have significant deviations and may even not agree within the uncertainties. Since the BNN-I5 is trained with the evaluated data, its pre-

dictions generally agree well with the experimental data that match within the errors, while falling between the experimental data when they do not agree within the errors. There is generally a large number of experimental cross sections near $E = 14.5$ MeV; it is found that the BNN-I5 predictions are close to the average value of the experimental data from different groups. In the future, we will try to directly learn those experimental data that match within the errors and then make predictions of cross sections where the data do not match within errors. It would be valuable to further explore which measurements the neural network predictions favored, thus providing reference values for the evaluation of experimental data.

Figure 10 shows the rms deviations of the BNN-I5 cross section predictions from the evaluation data for various nuclei. It is clear that the rms deviations of the BNN-I5 predictions are generally smaller than 0.1 barns for the light nuclei with $Z \lesssim 40$ and the heavy nuclei with $Z \gtrsim 80$. For nuclei with $40 \lesssim Z \lesssim 80$, the rms deviations of BNN-I5 are relatively larger, which are only within about 0.15 barns. However, the prediction accuracy of BNN-I5 is still better than that of TENDL-2021 in this region, as shown in Fig. 5. These medium mass nuclei have very complex nuclear structure phenomena, e.g., complex evolutions of nuclear shapes, spins, and parities, which could affect the $(n, 2n)$ reaction cross sections. These microscopic effects are very challenging for various machine learning methods, and therefore the BNN-I5 approach gives a relatively poor description of the $(n, 2n)$ cross section in this region. Including more physics into machine learning methods effectively improves their performance.

IV. SUMMARY AND PERSPECTIVES

In summary, the nuclear $(n, 2n)$ reaction cross sections and their uncertainties are predicted by the BNN approach. Three physical quantities besides Z and N , that is ΔE , δ , and σ^{th} , are identified as the best neural network inputs to describe the $(n, 2n)$ reaction excitation function. The BNN approach describes the $(n, 2n)$ reaction cross sections better than the TENDL-2021, not only for the small cross sections but also

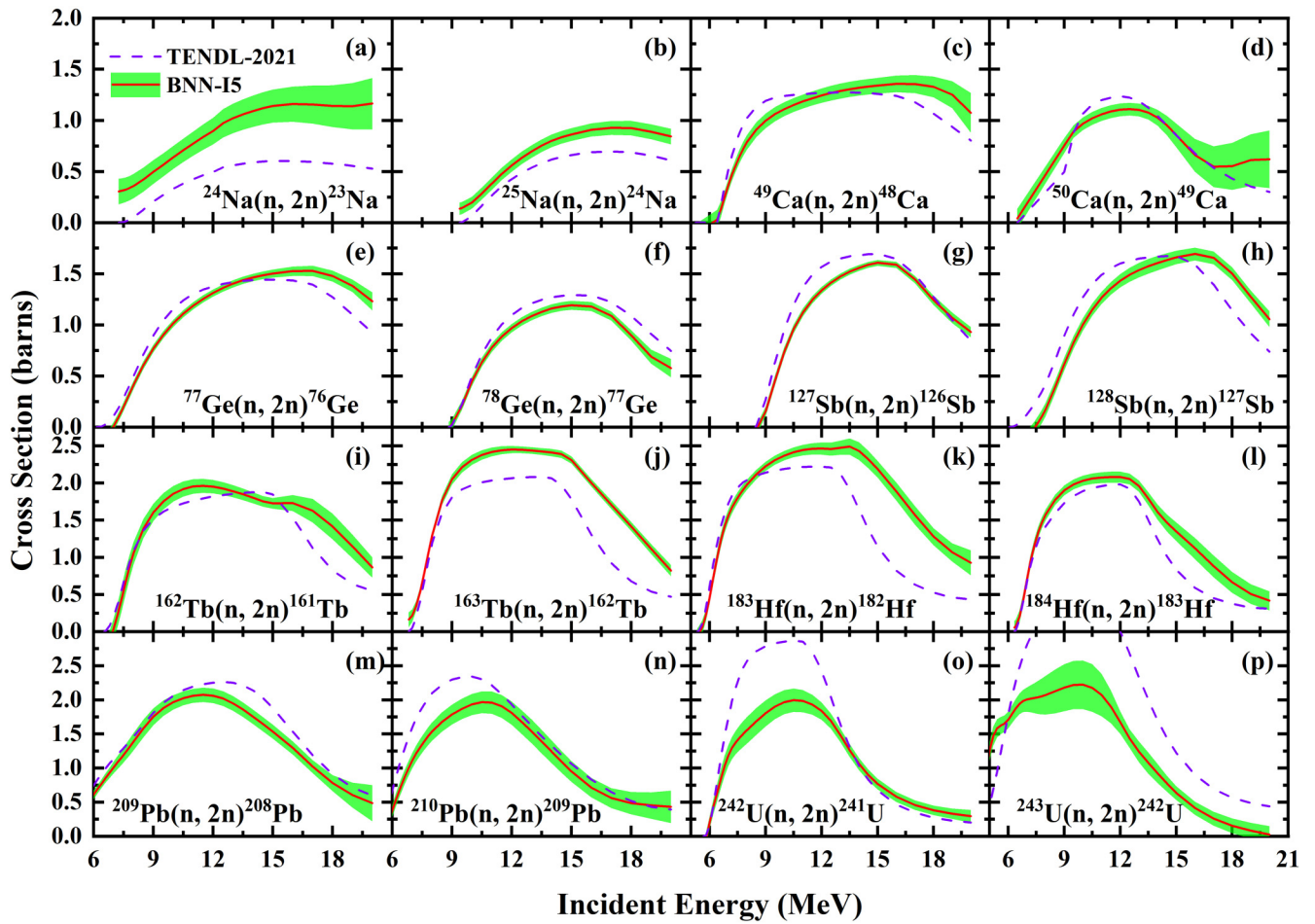


FIG. 8. Comparison of the $(n, 2n)$ reaction cross sections from BNN-I5 predictions and TENDL-2021 [66] for various nuclei.

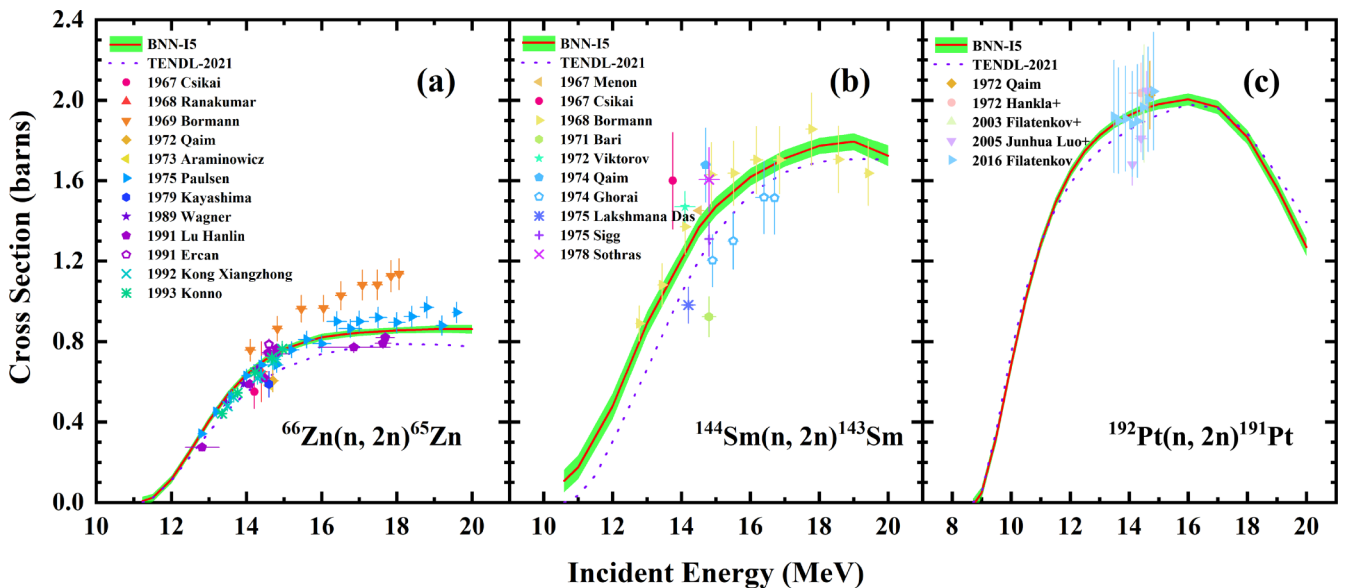


FIG. 9. Comparison of the $(n, 2n)$ reaction cross sections from BNN-I5 predictions with the original experimental data in Refs. [67–91] for ^{66}Zn , ^{144}Sm , and ^{192}Pt .

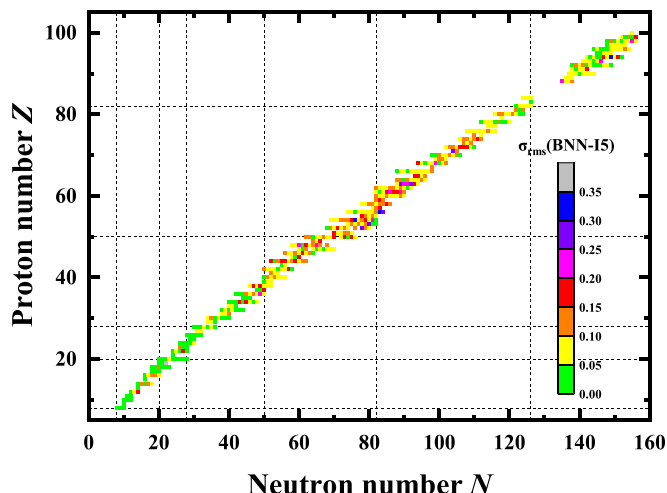


FIG. 10. The rms deviations between the $(n, 2n)$ reaction cross sections predicted by the BNN-I5 approach and evaluation data for various nuclei.

for the large cross sections. The rms deviation of the BNN approach with respect to the evaluation data is reduced to 0.10 barns compared to 0.25 barns of the TENDL-2021. The extrapolation ability of the BNN approach is verified with the $(n, 2n)$ cross section data that are not used to train the neural network. When extrapolated to the unknown region, the BNN approach can still well describe the trend of first increasing and then decreasing for the $(n, 2n)$ reaction exci-

tation functions with the incident neutron energy predicted by TENDL-2021. It is worth mentioning that in the heavy nuclear region the BNN approach may describe the $(n, 2n)$ reaction cross sections better than TENDL-2021, since the deviations between the TENDL-2021 predictions and the evaluation data become larger and larger for heavier nuclei, while the BNN approach has a similar prediction accuracy in the whole nuclear region. In addition, the BNN approach is consistent with the original experimental data of the $(n, 2n)$ reaction, especially the experimental cross sections near $E = 14.5$ MeV. The constructed neural network acquires the intrinsic patterns of the $(n, 2n)$ reaction cross sections by learning large-scale evaluation data and has some extrapolation ability, which can be used as an aid for nuclear data evaluation. In the future, various machine learning methods including the BNN will be extended to more reaction channels to find the features associated with the cross sections, thus providing a more reliable basis for large-scale nuclear data evaluation studies.

ACKNOWLEDGMENTS

We are grateful to Prof. H. Liang for fruitful discussions. This work was partly supported by the National Key Research and Development (R&D) Program under Grant No. 2021YFA1601500, the National Natural Science Foundation of China under Grants No. 12375109, No. 11875070, No. 11935001, and No. 12105369, the Anhui project (No. Z010118169), and the Key Research Foundation of Education Ministry of Anhui Province under Grant No. 2023AH050095.

- [1] P. Dimitriou, in *26th International Nuclear Physics Conference*, 11–16 September 2016, Adelaide [[PoS INPC2016, 118 \(2017\)](#)].
- [2] S. M. Qaim, [Nucl. Med. Biol.](#) **44**, 31 (2017).
- [3] M. S. Smith, [Nucl. Phys. A](#) **718**, 339 (2003).
- [4] J. Luo, J. Liang, L. Jiang, F. Tuo, L. He, L. Zhou, and Q. Yan, [Eur. Phys. J. A](#) **58**, 142 (2022).
- [5] K. Kolos, V. Sobes, R. Vogt, C. E. Romano, M. S. Smith, L. A. Bernstein, D. A. Brown, M. T. Burkey, Y. Danon, M. A. Elsayi *et al.*, [Phys. Rev. Res.](#) **4**, 021001 (2022).
- [6] J. Luo and L. Jiang, [Eur. Phys. J. A](#) **55**, 27 (2019).
- [7] E. Georgali, N. Patronis, A. Anastasiadis, X. Aslanoglou, M. Axiotis, Z. Eleme, S. Harissopoulos, A. Kalamara, K. Karpopoulos, M. Kokkoris *et al.*, [Phys. Rev. C](#) **102**, 034610 (2020).
- [8] N. S. Tawade, S. Patra, R. Tripathi, H. Kumawat, T. Patel, and P. K. Pujari, [Eur. Phys. J. A](#) **58**, 80 (2022).
- [9] M. Mehta, N. L. Singh, R. Singh, R. Chauhan, R. Makwana, S. V. Suryanarayana, H. Naik, P. V. Subhash, S. Mukherjee, J. Varmuza, and K. Katovsky, [Appl. Radiat. Isot.](#) **182**, 110142 (2022).
- [10] V. D. Bharud, F. M. D. Attarb, S. S. Dahiawalea, S. D. Dholea, and V. N. Bhoraskar, [Appl. Radiat. Isot.](#) **146**, 10 (2019).
- [11] A. Gandhi, A. Sharma, A. Kumar, R. Pachuau, B. Lalremruata, S. V. Suryanarayana, L. S. Danu, T. Patel, S. Bishnoi, and B. K. Nayak, [Phys. Rev. C](#) **102**, 014603 (2020).
- [12] H. B. Sachhidananda, S. R. Manohara, A. M. Sunitha, I. Pasha, B. Rudraswamy, S. V. Suryanarayana, H. Naik, M. Karkera, Y. S. Sheela, and M. Prasad, [J. Radioanal. Nucl. Chem.](#) **325**, 885 (2020).
- [13] R. K. Singh, N. L. Singh, R. D. Chauhan, M. Mehta, S. V. Suryanarayana, R. Makwana, B. K. Nayak, H. Naik, T. N. Nag, and K. Katovsky, [Chin. Phys. C](#) **46**, 054002 (2022).
- [14] V. Méot, O. Roig, B. Laurent, P. Morel, J. Aupiais, O. Delaune, G. Haouat, and O. Bouland, [Phys. Rev. C](#) **103**, 054609 (2021).
- [15] N. Otuka, E. Dupont, V. Semkova, B. Pritychenko, A. I. Blokhin, M. Aikawa, S. Babykina, M. Bossant, G. Chen, S. Dunaeva *et al.*, [Nucl. Data Sheets](#) **120**, 272 (2014).
- [16] V. V. Zerkin and B. Pritychenko, [Nucl. Instrum. Methods Phys. Res., Sect. A](#) **888**, 31 (2018).
- [17] A. D. Carlson, V. G. Pronyaev, R. Capote, G. M. Hale, Z. P. Chen, I. Duran, F. J. Hamsch, S. Kunieda, W. Mannhart, B. Marcinkevicius *et al.*, [Nucl. Data Sheets](#) **148**, 143 (2018).
- [18] D. A. Brown, M. B. Chadwick, R. Capote, A. C. Kahler, A. Trkov, M. W. Herman, A. A. Sonzogni, Y. Danon, A. D. Carlson, M. Dunn *et al.*, [Nucl. Data Sheets](#) **148**, 1 (2018); Evaluated Nuclear Data File (ENDF) database version of 2023-08-23, <https://www-nds.iaea.org/exfor/endl.htm>
- [19] A. J. M. Plompen, O. Cabellos, C. D. S. Jean, M. Fleming, A. Algora, M. Angelone, P. Archier, E. Bauge, O. Bersillon, A. Blokhin *et al.*, [Eur. Phys. J. A](#) **56**, 181 (2020).
- [20] O. Iwamoto, N. Iwamoto, S. Kunieda, F. Minato, S. Nakayama, Y. Abe, K. Tsubakihara, S. Okumura, C. Ishizuka, T. Yoshida *et al.*, [J. Nucl. Sci. Technol.](#) **60**, 1 (2023).

- [21] Z. Ge, R. Xu, H. Wu, Y. Zhang, G. Chen, Y. Jin, N. Shu, Y. Chen, X. Tao, Y. Tian *et al.*, *EPJ Web Conf.* **239**, 09001 (2020).
- [22] A. I. Blokhin, E. V. Gai, A. V. Ignatyuk, I. I. Koba, V. N. Manokhin, and V. G. Pronyaev, *Vopr. At. Nauki Tekh. Ser. Yad. Konstanty* **2**, 62 (2016).
- [23] A. J. Koning, S. Hilaire, and M. C. Duijvestijn, in *Proceedings, International Conference on Nuclear Data for Science and Technology*, 22–27 April 2007, Nice (EDP Sciences, Le Ulis, France, 2007), p. 211.
- [24] M. Herman, R. Capote, B. V. Carlson, P. Obložinský, M. Sin, A. Trkov, H. Wienke, and V. Zerkin, *Nucl. Data Sheets* **108**, 2655 (2007).
- [25] O. Iwamoto, *J. Nucl. Sci. Technol.* **44**, 687 (2007).
- [26] J. Zhang, *Nucl. Sci. Eng.* **142**, 207 (2002).
- [27] R. Capote, D. L. Smith, and A. Trkov, *EPJ Web Conf.* **8**, 04001 (2010).
- [28] V. Mnih, K. Kavukcuoglu, D. Silver, A. A. Rusu, J. Venness, M. G. Bellemare, A. Graves, M. Riedmiller, A. K. Fidjeland, G. Ostrovski *et al.*, *Nature (London)* **518**, 529 (2015).
- [29] P. Baldi, P. Sadowski, and D. Whiteson, *Nat. Commun.* **5**, 4308 (2014).
- [30] L. G. Pang, K. Zhou, N. Su, H. Petersen, H. Stöcker, and X. N. Wang, *Nat. Commun.* **9**, 210 (2018).
- [31] J. Brehmer, K. Cranmer, G. Louppe, and J. Pavez, *Phys. Rev. Lett.* **121**, 111801 (2018).
- [32] J. Carrasquilla and R. G. Melko, *Nat. Phys.* **13**, 431 (2017).
- [33] G. Carleo and M. Troyer, *Science* **355**, 602 (2017).
- [34] F. Villaescusa-Navarro, D. Anglés-Alcázar, S. Genel, D. N. Spergel, R. S. Somerville, R. Dave, A. Pillepich, L. Hernquist, D. Nelson, P. Torrey *et al.*, *Astrophys. J.* **915**, 71 (2021).
- [35] F. Villaescusa-Navarro, S. Genel, D. Angles-Alcazar, L. Thiele, R. Dave, D. Narayanan, A. Nicola, Y. Li, P. Villanueva-Domingo, B. Wandelt *et al.*, *Astrophys. J. Suppl. Ser.* **259**, 61 (2022).
- [36] W. B. He, Q. F. Li, Y. G. Ma, Z. M. Niu, J. C. Pei, and Y. X. Zhang, *Sci. China Phys. Mech. Astron.* **66**, 282001 (2023).
- [37] Z. P. Gao, Y. J. Wang, H. L. Lu, Q. F. Li, C. W. Shen, and L. Liu, *Nucl. Sci. Tech.* **32**, 109 (2021).
- [38] X. H. Wu, L. H. Guo, and P. W. Zhao, *Phys. Lett. B* **819**, 136387 (2021).
- [39] X. H. Wu, Y. Y. Lu, and P. W. Zhao, *Phys. Lett. B* **834**, 137394 (2022).
- [40] Z. M. Niu, Z. L. Zhu, Y. F. Niu, B. H. Sun, T. H. Heng, and J. Y. Guo, *Phys. Rev. C* **88**, 024325 (2013).
- [41] J. S. Zheng, N. Y. Wang, Z. Y. Wang, Z. M. Niu, Y. F. Niu, and B. Sun, *Phys. Rev. C* **90**, 014303 (2014).
- [42] Z. M. Niu, B. H. Sun, H. Z. Liang, Y. F. Niu, and J. Y. Guo, *Phys. Rev. C* **94**, 054315 (2016).
- [43] Y. F. Ma, C. Su, J. Liu, Z. Z. Ren, C. Xu, and Y. Gao, *Phys. Rev. C* **101**, 014304 (2020).
- [44] D. Wu, C. L. Bai, H. Sagawa, and H. Q. Zhang, *Phys. Rev. C* **102**, 054323 (2020).
- [45] N. N. Ma, X. J. Bao, and H. F. Zhang, *Chin. Phys. C* **45**, 024105 (2021).
- [46] Z. Y. Yuan, D. Bai, Z. Z. Ren, and Z. Wang, *Chin. Phys. C* **46**, 024101 (2022).
- [47] N. J. Costiris, E. Mavrommatis, K. A. Gernoth, and J. W. Clark, *Phys. Rev. C* **80**, 044332 (2009).
- [48] S. Akkoyun, H. Kaya, and Y. Torun, *Indian J. Phys.* **96**, 1791 (2022).
- [49] R. D. Lasserri, D. Regnier, J. P. Ebran, and A. Penon, *Phys. Rev. Lett.* **124**, 162502 (2020).
- [50] S. Akkoyun and N. Amrani, *Radiat. Phys. Chem.* **184**, 109445 (2021).
- [51] M. A. B. Hamid, H. G. Beh, N. N. S. Nidzam, X. Y. Chew, and S. Ayub, *Appl. Radiat. Isot.* **187**, 110306 (2022).
- [52] H. Özdoğan, Y. A. Üncü, M. Şekerci, and A. Kaplan, *Appl. Radiat. Isot.* **192**, 110609 (2023).
- [53] S. Akkoyun, N. Amrani, and T. Bayram, *Appl. Radiat. Isot.* **191**, 110554 (2023).
- [54] Z. M. Niu and H. Z. Liang, *Phys. Lett. B* **778**, 48 (2018).
- [55] L. Neufcourt, Y. Cao, W. Nazarewicz, and F. Viens, *Phys. Rev. C* **98**, 034318 (2018).
- [56] U. B. Rodríguez, C. Z. Vargas, M. Gonçalves, S. B. Duarte, and F. Guzmán, *Europhys. Lett.* **127**, 42001 (2019).
- [57] Z. M. Niu, J. Y. Fang, and Y. F. Niu, *Phys. Rev. C* **100**, 054311 (2019).
- [58] Z. M. Niu and H. Z. Liang, *Phys. Rev. C* **106**, L021303 (2022).
- [59] R. Utama, W. C. Chen, and J. Piekarewicz, *J. Phys. G: Nucl. Part. Phys.* **43**, 114002 (2016).
- [60] Y. L. Yang and P. W. Zhao, *Phys. Rev. C* **107**, 034320 (2023).
- [61] Z. M. Niu, H. Z. Liang, B. H. Sun, W. H. Long, and Y. F. Niu, *Phys. Rev. C* **99**, 064307 (2019).
- [62] Y. F. Wang, X. Y. Zhang, Z. M. Niu, and Z. P. Li, *Phys. Lett. B* **830**, 137154 (2022).
- [63] Z. A. Wang, J. Pei, Y. Liu, and Y. Qiang, *Phys. Rev. Lett.* **123**, 122501 (2019).
- [64] C. Y. Qiao, J. C. Pei, Z. A. Wang, Y. Qiang, Y. J. Chen, N. C. Shu, and Z. G. Ge, *Phys. Rev. C* **103**, 034621 (2021).
- [65] W. F. Li, X. Y. Zhang, Y. F. Niu, and Z. M. Niu, *J. Phys. G: Nucl. Part. Phys.* **51**, 015103 (2024).
- [66] A. J. Koning, D. Rochman, J. Sublet, N. Dzysiuk, M. Fleming, and S. van der Marck, *Nucl. Data Sheets* **155**, 1 (2019); Evaluated Nuclear Data File (ENDF) database version of 2023-08-23, <https://www-nds.iaea.org/exfor/endl.htm>.
- [67] J. Csikai, and G. Pető, *Acta. Phys. Hung.* **23**, 87 (1967).
- [68] N. Ranakumar, E. Kondaiah, and R. W. Fink, *Nucl. Phys. A* **122**, 679 (1968).
- [69] M. Bormann and B. Lammers, *Nucl. Phys. A* **130**, 195 (1969).
- [70] S. M. Qaim, *Nucl. Phys. A* **185**, 614 (1972).
- [71] J. Araminowicz and J. Dresler, Inst. Badan Jadr. (Nucl. Res.), Swierk + Warsaw, Report No. 1464, 1973 (unpublished), p. 14.
- [72] A. Paulsen, H. Liskien, and R. Widera, *Atomkernenergie* **26**, 34 (1975).
- [73] K. Kayashima, A. Nagao, and I. Kumabe, Japanese Report to the I.N.D.C., No. 47, 1979 (unpublished), p. 94.
- [74] M. Wagner, G. Winkler, H. Vonach, Cs. M. Buczko, and J. Csikai, *Ann. Nucl. Energy* **16**, 623 (1989).
- [75] H. Lu, W. Zhao, and W. Yu, *Chin. J. Nucl. Phys.* **13**, 11 (1991).
- [76] A. Ercan, M. N. Erduran, M. Subasi, E. Gueltekin, G. Tarcan, A. Baykal, and M. Bostan, in *Nuclear Data for Science and Technology*, Proceedings of an International Conference, held at the Forschungszentrum Jülich, Fed. Rep. of Germany, 13–17 May 1991, edited by S. M. Qaim (Springer, Berlin, 1992), p. 376.
- [77] X. Kong, Y. Wang, J. Yuan, J. Yang, and Y. Shui, Lanzhou Univ., *Nat. Sci. Ed.* **28**, 99 (1992).

- [78] C. Konno, Y. Ikeda, K. Oishi, K. Kawade, H. Yamamoto, and H. Maekawa, JAERI Report No. 1329, 1993 (unpublished).
- [79] M. P. Menon and M. Y. Cuypers, *Phys. Rev.* **156**, 1340 (1967).
- [80] M. Bormann, A. Behrend, I. Riehle, and O. Vogel, *Nucl. Phys. A* **115**, 309 (1968).
- [81] A. Bari, *Diss. Abstr. Int. B, Sci. Eng.* **32**, 5091 (1972).
- [82] D. V. Viktorov and V. L. Zyablin, *Sov. J. Nucl. Phys.* **15**, 608 (1972).
- [83] S. M. Qaim, *Nucl. Phys. A* **224**, 319 (1974).
- [84] S. K. Ghorai, R. Vos, J. R. Cooper, and W. L. Alford, *Nucl. Phys. A* **223**, 118 (1974).
- [85] N. Lakshmana Das, C. V. Srinivasa Rao, B. V. Thirumala Rao, and J. Rama Rao, in *Proceedings of the Nuclear Physics and Solid State Physics Symposium 1965* (India Department of Atomic Energy, New Delhi, 1975).
- [86] R. A. Sigg and P. K. Kuroda, *J. Inorg. Nucl. Chem.* **37**, 631 (1975).
- [87] S. L. Sothras and G. N. Salaita, *J. Inorg. Nucl. Chem.* **40**, 585 (1978).
- [88] A. K. Hankla, R. W. Fink, and J. H. Hamilton, *Nucl. Phys. A* **180**, 157 (1972).
- [89] A. A. Filatenkov and S. V. Chuvae, Khlopin Radiev. Inst. Leningrad Report No. 259, 2003 (unpublished).
- [90] J. Luo, G. He, Z. Liu, and X. Kong, *Radiochim. Acta* **93**, 381 (2005).
- [91] A. A. Filatekov, USSR Report to the I.N.D.C., No. 0460, 2016, <https://www-nds.iaea.org/publications/indc/indc-ccp-0460/>.